Materials Today: Proceedings 92 (2023) 933–937

Contents lists available at ScienceDirect

Materials Today: Proceedings

journal homepage: www.elsevier.com/locate/matpr

Nano NaA thick film: Excellent EG vapors sensor

Malikarjun D. Wakade [a,b], Kishori B.Naik [b], Vikas D. Kutte [b], Vijaykiran N. Narwade [c], Madhuri A. Lakhane [d], Kashinath A. Bogle [b], Rajendra S. Khairnar [b], Megha P. Mahabole [b,*]

[a] Shivneri Mahavidyalaya, Shirur Anantpal, Dist. Latur 413544, MS, India
[b] School of Physical Sciences, S.R.T.M. University, Nanded 431606, MS, India
[c] RUSA-Centre for Advanced Sensor Techkogy, Dr. B.A.M.University, Aurangabad 431001, MS, India
[d] D.S.M. College, Prabhani 431401, MS, India

ARTICLE INFO

Article history:
Available online 9 May 2023

Keywords:
Nano Sodium A zeolite
Ethylene Glycol sensor
Thick film
Screen printig techniques
XRD

ABSTRACT

The aim of the present research is to use a thick film of Nano Sodium A Zeolite (NaA) sensors to detect ethylene glycol vapours (EG). The obtained NaA zeolite material was characterised using XRD, FTIR, SEM-EDS, and TG-DTA analysis to investigate its physicochemical properties. The screen printing technique was used to deposit NaA thick films on glass substrates. NaA sensors have been found to be sensitive to EG. The sensors were revealed to functional operating temperature at 95 °C, with fast response and recovery times of 90 s, respectively. EG vapours with concentrations ranging from 2 to 90 ppm can be detected by the sensors. According to the findings, NaA zeolite could be used as a potential method for identifying EG vapours..

Selection and peer-review under responsibility of the scientific committee of the 2nd International Conference on Multifunctional Materials.

1. Introduction

Air pollution has rapidly increased during the last few years due to industrial and technological development and is becoming one of the large as worldwide nightmares as it destructively affects ecosystem [1–3]. Air pollutants are not only hazardous but also disadvantageous to the environment. Their presence, in massive concentration, leads to global warming, acid rain, smog and can cause adverse effect on living organism [4]. Therefore, there is a need of appropriate system to take the edge off such problem to detect hazardous and harmful air pollutants in order to protect human health.

Ethylene glycol (EG) is the most basic organic chemical in the glycol family with two hydroxyl groups in adjacent positions in a hydrocarbon chain. Ethylene glycol is a clear, colourless, odourless liquid that is relatively non-volatile and viscous [5]. It is also widely used as a raw material for antifreeze, coolants, dyes, inks, plastics, paints, films, solar energy systems, hydraulic break fluids, cosmetics, thus as used divase fields like medical, automotive, petrochemical, mechanical, pharmaceutical, and printing press industries. EG vapours, on the other hand, are highly toxic and can harm human health. Inhaling EG vapors can cause respiratory problems, pulmonary edoema, and damage to nervous system, heart, and kidneys. Furthermore, EG vapour exposure results in CNS depression, nausea, vomiting, abdominal cramps, coma, minor skin and ocular irritation, and even death. EG can also cause cancer. Detecting and monitoring EG vapours is thus critical for human safety [6]. Detection of EG vapours has rarely been reported in the literature to date. As a result, it is nessary to develop can detect these vapours efficiently [7].

Recently nano materials have gained much interest in sensor applications because of their interesting features like increase in surface to volume ratio, high adsorption capacity and reactivity. In this context, nano-zeolites are very interesting materials which are widely being used in many areas ranging from catalysis, chromatography, medical, agricultural, veterinary, ion exchange, waste management and specially gas sensing applications [8,9]. The reviews on utilization of zeolites for sensor application indicate that most of the zeolites either in layer form, or admixtures or composites are employed for augmentation of sensor performance towards toxic gases. [10–12]. In addition, they have not been used to detect EG vapours.

Zeolite A with sodium cations, $[Na_{12}[(AlO_2)_{12}(SiO_2)_{12}].27H_2O$, abbreviated as NaA], is a microporous aluminosilicate material. Its unique structure contains molecular-sized crystalline, void

* Corresponding author.
E-mail address: mpmsrtmunsps@gmail.com (M.P. Mahabole).

https://doi.org/10.1016/j.matpr.2023.04.546
2214-7853/
Selection and peer-review under responsibility of the scientific committee of the 2nd International Conference on Multifunctional Materials.

spaces, channels and cages [8]. It is due to its intra-crystalline surface area and strong interactions with adsorbates, it exhibits molecular-sieving, catalytic, ion-exchange and adsorption properties. NaA zeolite material, its membranes and composites are mainly employed for adsorption of radioactive waste, removal of heavy metals, oil–water separation, gas separation, catalysis and carbon dioxide capture [10], There are very few reports on sensor application wherein NaA layer or NaA composite have been used for improvement either in selectivity or sensitivity [10–12].

Furthermore, the use of NaA zeolite for EG vapour recognition has yet to be reported. As a result, efforts have been made to develop a thick film sensor based on NaA zeolite for detecting EG vapours. Hence, the present work deals with utilization of nano-NaA zeolite for detection EG vapours. It includes preparation of thick film sensors by using nano-NaA zeolite as main functional material, characterization of sensor material and detail EG vapour sensing characteristics.

2. Experimental

Nano-NaA zeolite and ethylene glycol were procured from Merck with high purity level up 99.9 % and S.D. Fine Chemicals Limited (SDFCL) respectively.

2.1. Characterization

The X-ray diffraction patterns has obtained using a Rigaku X-ray diffractometer (Miniflex) and CuKa (=1.543) incident radiation. The XRD peaks were measured between 5° and 60°. The functional groups in the NaA zeolite were identified using a Perkin-Elmer Shimadzo FTIR spectrophotometer. The sample was scanned 50 times from 4000 $cm^{-1}$to 400 cm^{-1}. The spectrometer with a resolution of 4 cm^{-1}.

Shimadzu Thermal analyzer was used to perform thermogravimetric and differential thermal analysis in an air atmosphere at a rate of 10 °C/min its temperature range from room temperature to 1400 °C.

2.2. Preparation of thick films

The thick film sensors were obtained using the previously described screen-printing technique [13,14]. A paste was prepared using NaA zeolite as a main functional material and various binders namly glass frit, ethyl cellulose and butyl carbitol acetate by keeping inorganic to organic ratio 70:30 and deposited on the clean glass substrate. After deposition, the films were dried for 20 min under an infrared lamp to remove temporary binders before being annealed in air for 2 h at 650 °C in a programmable furnace. These newly developed screen printed thick film sensors were used to detect EG vapours. The process of film preparation is presented in Fig. 1.

2.3. EG vapour sensing performance

A study on the detection of EG vapours was conducted using a labmade static gas assembly. A sensor substrate was mounted on a heater in the chamber and a constant voltage of 90 V was applied. The temperature of the substrate was determined by placing a thermocouple in direct contact with it. To enable electrical measurements, the copper electrodes were connected to the substrate material. To avoid the humidity consequences and maintain a consistent output, the sensor substrate was heated in atmospheric air. The DC electrical resistance of a NaA zeolite thick film sensor as a function of temperature in air and air with test vapour environments was calculated. Using the observed change in resistance, the sensitivity of the sensor film was calculated using following equation.

$$GasresponseS(\%) = \frac{R_{gas} - R_{air}}{R_{air}} \times 100$$

The repeatability of the sample film was assessed three times while measuring gas response as a function of temperature [15]. The response and recovery times of the film were also determined by alternately exposing them to a constant (EG vapour concentration) and a fresh air environment. The active region of the film sensor was studied by exposing it to varying concentrations of EG vapours while the sensor keeping at its working temperature.

3. Results and discussion

3.1. X-ray diffraction analysis

Fig. 2(a) depicts the diffraction pattern of NaA zeolite from 10° to 60°. Typical NaA zeolite patterns includes diffraction peaks at 2θ values of 10.190, 12.480, 16.130, 21.680, 24.010, 26.150, 27.150, 29.960, 30.80, 32.50, 34.10, 35.70, and 41.50 (74–1183-JCPDS-ICDD, 2001). The planes (531), (662), (640), (642), (644), (660), (840), and (880) correspond to the NaA zeolite's tetragonal phase. Calculating the average particle size of NaA zeolite is found to be 66 nm [16].

3.2. Fouriour transform infrared spectroscopy

Fig. 2(b) shows the FTIR spectrum of NaA zeolite material recorded between 400 and 4000 cm^{-1}. The distinctive band for NaA zeolite framework, which is present at 664 cm^{-1}, is caused by the internal vibration of T-O symmetric stretching. The absorption peak associated with asymmetric stretching vibrations of Si-O (Si) and Si-O(Al) bridge bonds is discovered to be close to 1005 cm^{-1}. Internal tetrahedral symmetrical stretching has a peak at 1497 cm^{-1} and external linkage asymmetrical stretching has a peak at 1648 cm^{-1}. The peak at 2360 cm^{-1} is caused by internal (TO_4) tetrahedral bending. The absorption band of the (OH) group is found to be present at 3733 cm^{-1} [17].

3.3. Thermo-gravitometric and diffrential theramal analysis

The TG (blue) and DTA (black) curves for NaA zeolite are shown in Fig. 2c. The initial weight loss in the temperature range of 50 °C to 200 °C indicates water molecule desorption from the zeolite surface. The first endothermic peak at around 65 °C, caused by the desorption of loosely held water molecules in the NaA zeolite, supports this. Dehydration of the hydrated sodium ions located in the cages of the zeolite framework causes the appearance of the second endothermic peak at 220 °C. Changes in the chemical composition of the NaA zeolite material are linked to the newly discovered exothermic peak at 400 °C [18].

3.4. Scanning electron microscopy and energy dissipative spectroscopy

Fig. 3(a) displays the SEM image of the NaA zeolite. The observed morphologies are similar to well-defined cubic crystals, as expected for highly crystalline NaA zeolite. This is well supported by sharp peaks in XRD [14]. The average elemental chemical composition of the NaA sample, obtained quantitatively from energy dispersive analysis (EDS), is shown in Fig. 3(b). The EDS spectrum shows the presence of elements like Al, Na, C, O and Si. The abundance of Al and Si confirms that Si/Al ration is greater than 1 [19,20].

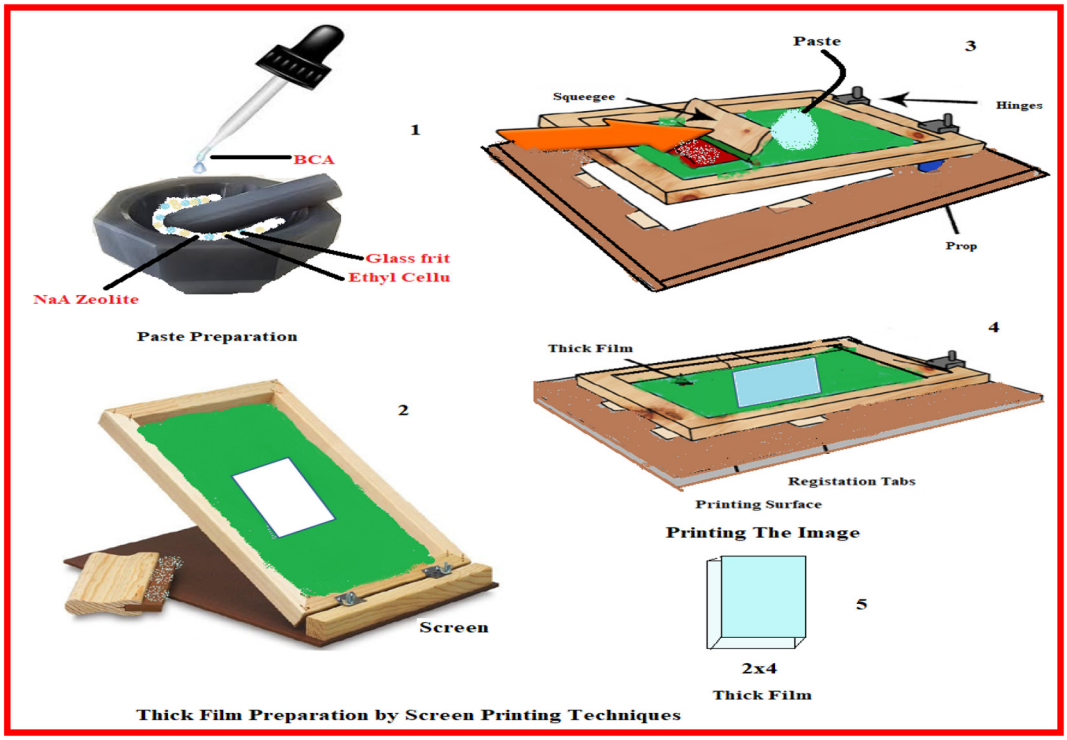

Fig. 1. Paste and Thick Film Preparation by Screen Printing Setup.

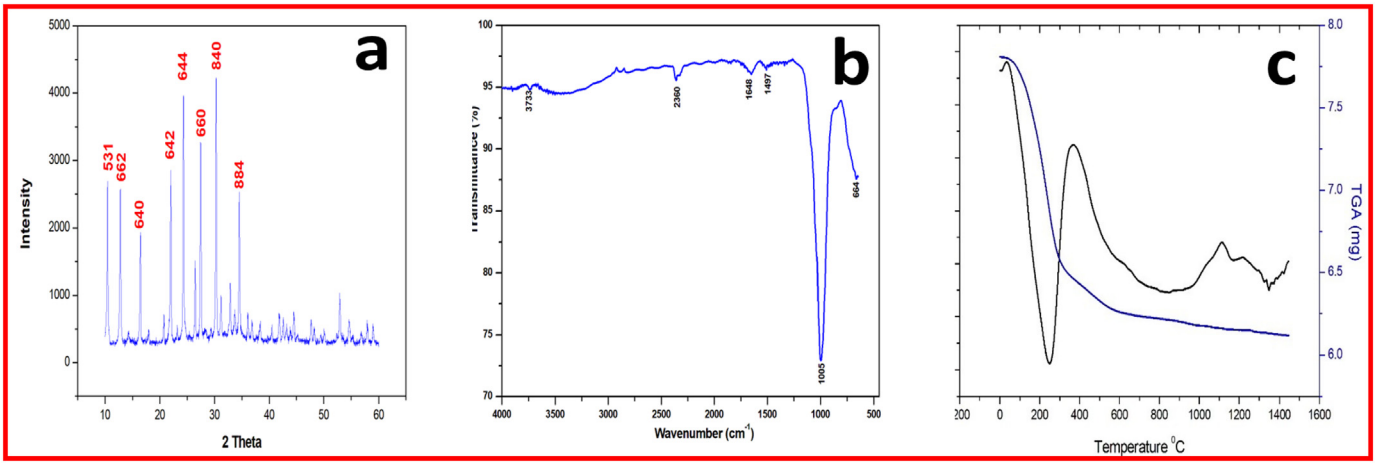

Fig. 2. A) XRD and b) FTIR and c) TG-DTA of Na A Zeolite sample.

3.5. Scanning electron microscopy and energy dissipative spectroscopy

Fig. 3(a) displays the SEM image of the NaA zeolite. The observed morphologies are similar to well-defined cubic crystals, as expected for highly crystalline NaA zeolite. This is well supported by sharp peaks in XRD [14]. The average elemental chemical composition of the NaA sample, obtained quantitatively from energy dispersive analysis (EDS), is shown in Fig. 3(b). The EDS spectrum shows the presence of elements like Al, Na, C, O and Si. The abundance of Al and Si confirms that Si/Al ration is greater than 1 [19,20].

3.6. Ethylene glycol sensing characteristics

Fig. 4(a) depicts the typical response of a NaA thick film sensor for a 2 ppm EG vapour as a function of temperature. It is observed that the sensitivity changes with temperature. The sensitivity is found to be maximum 166% at 95 °C. It demonstrates that the NaA film sensor has specific temperature sensitivity for EG vapours, as the response at all other temperatures is alimeage compared to that at 95 °C. This demonstrates that NaA thick film is an excellent EG vapour sensor, capable of detecting EG vapours at temperatures approaching 95 °C. The sensitivity for 2 ppm EG vapour concentration is 166%.

Fig. 4(b) depicts the response and recovery time profile for a NaA zeolite sensor in the presence of 2 ppm ethylene glycol vapours at 95 °C. The sensor's response is recorded alternately in the presence of atmospheric air and 2 ppm ethylene glycol vapour in atmospheric air. After a 2 ppm ethylene glycol injection, the sensor's response gradually increases until it reaches a constant value, which gives the sensor's response time. The time it takes for the sensor to return to its original value after being exposed to fresh

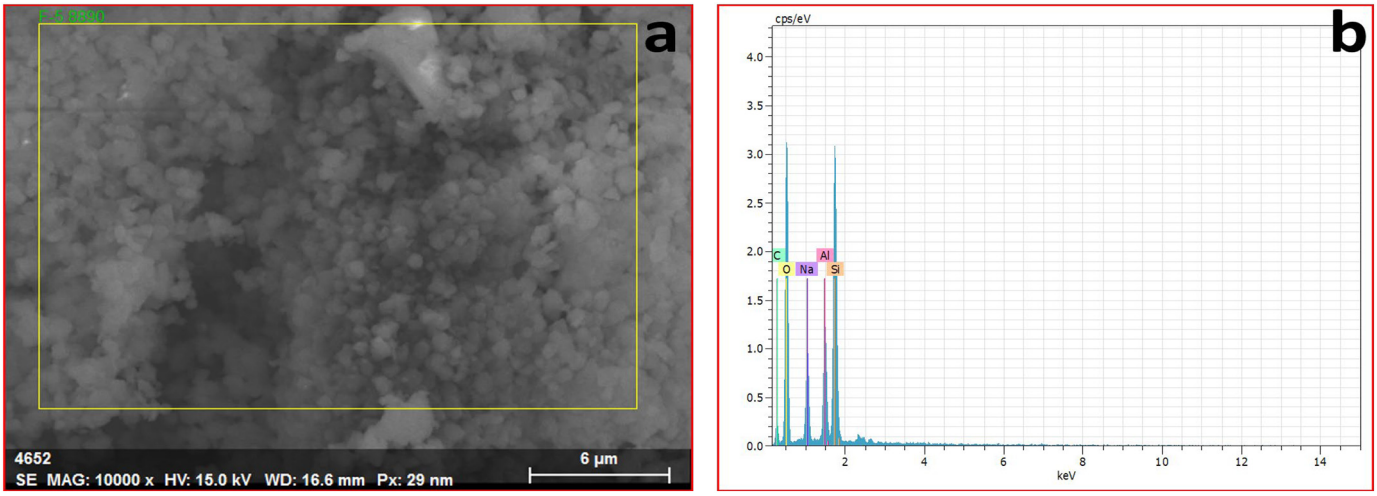

Fig. 3. (a) SEM images for Nano Sodium A Zeolite sample and (b) EDAX spectrum for Nano Sodium A Zeolite sample.

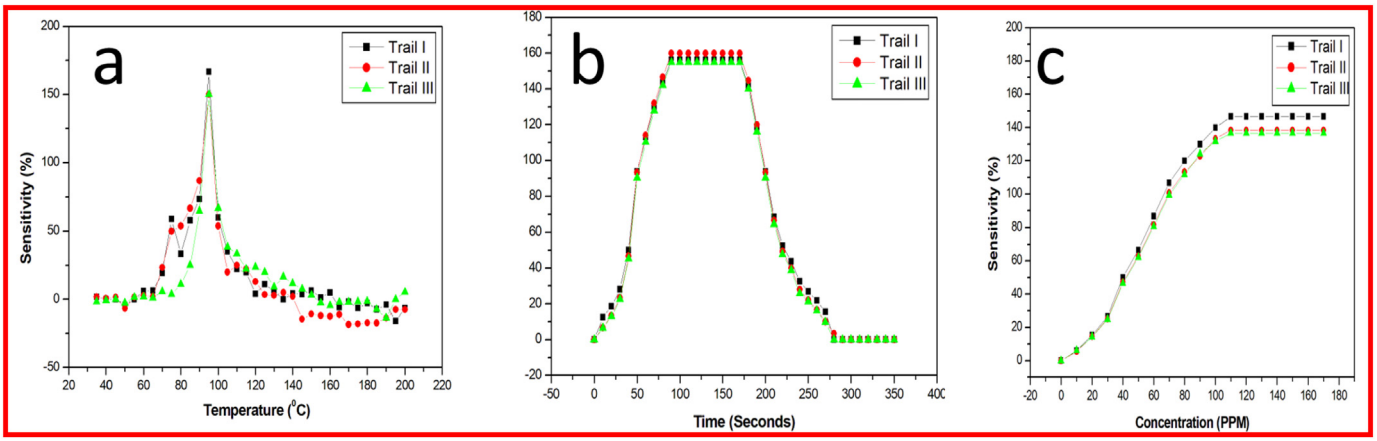

Fig. 4. A) eg vapors sensing ability of the naa substate as a function of time after exposing 2 ppm ethylene glycol concentration at optimum temperature (95 °C). b) Sensor sensitivity evaluated as the gas response v/s temperature of NaA substate in presence of EG vapors for 2 ppm to obtain optimum temperature. c) Maximum uptake capacity of EG vapors shown by nano NaA thick film at optimum temperature (95 °C).

air represents the sensor film's regenerative capacity and is referred to as recovery time. Based on the graph, it can be concluded that the NaA zeolite film responds to EG vapours in 90 s, with a recovery time of 90 s.

At 95 °C, the maximum uptake capacity of a NaA zeolite thick film sensor is investigated by varying the concentration of ethylene glycol vapour. Fig. 4(C) shows that the response almost linearly increases with concentration up to 90 ppm before becoming saturated for even higher concentrations it may be due to EG vapour coverage of the sensor surface. This finding shows that the NaA zeolite sensor can detect EG vapours at concentrations ranging from 2 to 90 ppm. Reveling the sensor's active range and detection capacity.

4. Gas sensing mechanism

NaA zeolite unit cell's aluminosilicate framework is made up of octahedrons (called cages) located at the eight corners of a cube and two cages are connected by a D4R linkage leading to the cube's edge. The diameter of an octahedron's (cage) is approximately 0.66 nm. Eight such interconnected octahedrons in a unit cell result in the formation of a slightly larger cavity (cage with a diameter of 1.14 nm.) as shown in Fig. 5.

Due to the combination of cages and connecting channels, zeolite offers extremely large specific surface area for the adsorbtion of foreign (EG) molecules. Any physical adsorption process involves Van der Waals dispersion-repulsion forces, as well as electrostatic forces caused by polarisation, dipole, and quadruple interactions. However, because zeolites have an ionic structure, electrostatic forces play an important role in molecule adsorption. Furthermore, in NaA zeolite, the zeolitic water molecules are loosely bound to the framework cations and can be found in the channels, cages, or voids. The water molecules in the structure obstruct the movement of mobile cations. Therefore, the ionic conductivity due to mobile cations is low at low temperatures. Zeolitic water desorption takeplace at higher temperatures. This results in rearrangement of chage carriers, and the adsorbed EG molecules can enter inside the zeolite structure. Thus rearrangement of chage carries result in high ionic movement increages conductivity. At 95 °C, this situation occurs in NaA zeolite, indicating that the maximum number of active adsorption sites occupied by ethylene glycol molecules. As a result, the response is observed to be the highest at this temperature. When exposed to low concentrations of EG vapours, the sensor responds very slowly due to the small surface coverage by EG vapour molecules (02 ppm). As the concentration of EG vapours increases, EG molecules occupy more surface area, and the response increases. A saturation stage occurs when all active sites are occupied. Thus, at higher concentrations, the response to ethylene glycol vapours becomes constant.

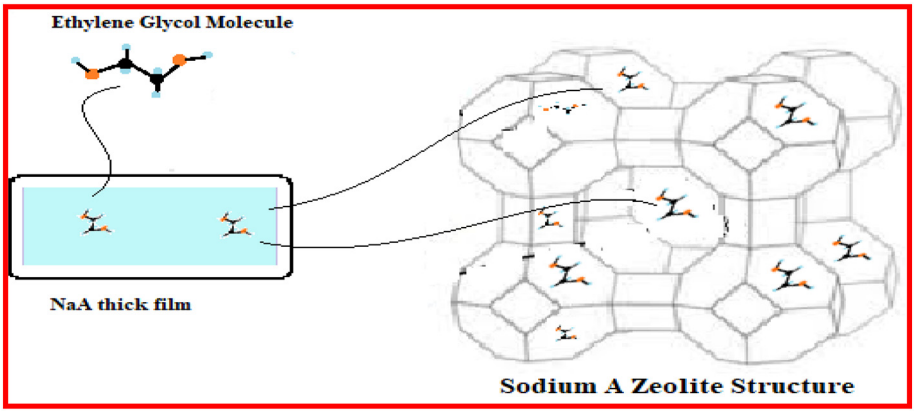

Fig. 5. Sensing Mechanism.

Then, adsorption of ethylene glycol molecules may occur when a nano-NaA zeolite film is exposed to ethylene glycol vapours due to the weaker interaction of ethylene glycol molecules with Bronsted active sites present at the zeolite surface. Thus, the Si-OH and Si-OH-Al grroups may be responsible for adsorption of EG on NaA zeolite film surface.

5. Conclusions

The structural, functional, theramal and morphological characteristics are carried out by means of XRD, FTIR, TG-DTA and SEM-EDS respectively. The experimental study of NaA film sensor is sensitive to EG vapours. The working temperature is at least 95 °C. The NaA sensor can detect EG vapours within 1.5 min and get back to normal within 1.5 min. A sensor can detect EG vapours with a minimum concentration of 2 ppm. NaA sensor exhibit a dynamic range of 2 ppm to 90 ppm for EG vapours.

CRediT authorship contribution statement

Kishori B.Naik: Data curation. **Vikas D. Kutte:** Formal analysis. **Vijaykiran N. Narwade:** Formal analysis. **Madhuri A. Lakhane:** Investigation. **Kashinath A. Bogle:** Methodology, Software. **Rajendra S. Khairnar:** Supervision, Validation. **Megha P. Mahabole:** Supervision, Writing – original draft, Writing – review & editing.

Data availability

No data was used for the research described in the article.

Declaration of Competing Interest

The authors declare the following financial interests/personal relationships which may be considered as potential competing interests: Megha P. Mahabole reports was provided by Swami Ramanand Teerth Marathwada University School of Physical Sciences. Dr. Vijaykiran N. Narwade reports formal analysis was provided by RUSA Center for Advanced Sensor Technology Dr Babasaheb Ambedkar Marathwada University. Malikarjun D. Wakade reports a relationship with Swami Ramanand Teerth Marathwada University School of Physical Sciences that includes: non-financial support. Kashinath A. Bogle has patent pending to no.

Acknowledgement

Authors would like to thank Hon. V.C., Swami Ramanand Teerth Marathwada Univesity, Nanded for constant support and encouragement.

References

[1] V.N. Narwade, S.R. Anjum, V. Kokol, R.S. Khairnar, Ammonia-sensing ability of differently structured hydroxyapatite blended cellulose nanofibril composite films, Cellulose 26 (5) (2019) 3325–3337.
[2] Ioannis Manisalidis, Elisavet Stavropoulou, Agathangelos Stavropoulos, Eugenia Bezirtzoglou, Environmental and Health Impacts of Air Pollution: A review, 2296-2565, doi:10.3389/fpubh.2020.00014.
[3] WHO Air pollution. Available from: http://www.who.int/airpollution/en/ cited Oct 5 2019.
[4] V.N. Narwade, Y.B. Pottathara, S. Begum, M.A. Lakhane, H.R. Tiyyagura, R.S. Khairnar, K.A. Bogle, Nanostructured hydroxyapatite biomaterial as gas sensor, in: Nanoscale Processing, Elsevier, 2021, pp. 439–466.
[5] H.C. Fuller, Ethylene glycol—its properties and uses, Ind. Eng. Chem. 16 (6) (1924) 624–626.
[6] S.C. Amstrup, C. Gardner, K.C. Meyers, F.W. Oehme, Ethylene glycol (antifreeze) poisoning in a free-ranging polar bear, Vet. Hum. Toxicol. 31 (4) (1989) 317–319.
[7] Wenjin Wan, Yuehua Li, Xingping Ren, Yinping Zhao, Fan Gao and Heyun Zhao. 2D SnO_2 Nanosheets: Synthesis, Characterization, Structures, and Excellent Sensing Performance to Ethylene Glycol Nanomaterials 2018, 8(2), 112
[8] Handbook of Zeolite Science and Technology, Scott M. Auerbach, Kathleen A. Carrado, Prabir K. Dutta, Marcel Dekker, Inc., New York, 2003.
[9] Review Applications of Zeolites in Sustainable Chemistry, Yi Li, Lin Li Jihong Yu, Chem, Volume 3, Issue 6, 14 December 2017, Pages 928-949
[10] Review Zeolite-based Materials for Gas Sensors Xiaowen Xu, Jing Wang and Yingcai Long, *Sensors* 2006, *6*, 1751-1764
[11] Y. Suna, J. Wanga, H. Dua, X. Lie, C. Wangb, T. Houb, Formaldehyde gas sensors based on SnO2/ZSM-5 zeolite composite nanofibers, J. Alloy. Compd. 868 (2021), https://doi.org/10.1016/j.jallcom.2021.159140.
[12] Eun Hye Kwon, Hyejin An, Min Bum Park, Min Kim, Yeong Don Park, Conjugated polymer–zeolite hybrids for robust gas sensors: Effect of zeolite surface area on NO_2 sensing ability, Chemical Engineering Journal, Volume 420, Part 1, 15 September 2021, 129588, https://doi.org/10.1016/j.cej.2021.129588
[13] M.P. Mahabole, M.A. Lakhane, A.L. Choudhari, R.S. Khairnar, Comparative study of natural calcium stilbite and magnesium exchanged stilbite for ethanol sensing, J. Porous Mater. 20 (4) (2013) 607–617.
[14] S.R. Anjum, V.N. Narwade, K.A. Bogle, R.S. Khairnar, Graphite doped Hydroxyapatite nanoceramic: selective alcohol sensor, Nano-Struct. Nano-Objects 14 (2018) 98–105.
[15] S. Taha, S. Begum, V.N. Narwade, D.I. Halge, J.W. Dadge, M.P. Mahabole, R.S. Khairnar, K.A. Bogle, Development of alcohol sensor using TiO2-Hydroxyapatite nano-composites, Mater. Chem. Phys. 240 (2020) 122228.
[16] R.S. Khairnar, M.D. Wakde, M.P. Mahabole, R. Krishna, E. Titus, Development of ethanol sensor using Sodium A nano zeolite, Int. J. Eng. Innov. Technol. (IJEIT) 3 (11) (May 2014).
[17] Włodzimierz MOZGAWA, Magdalena KRÓL, Katarzyna BARCZYK, FT-IR studies of zeolites from different structural groups, CHEMIK 2011, 65, 7, 667-674
[18] N.M. Musyoka, L.F. Petrik, E. Hums, A. Kuhnt, W. Schwieger, Thermal stability studies of zeolites A and X synthesized from South African coal fly ash, Res. Chem. Intermed. 41 (2) (2015) 575–582.
[19] Mohamed M.SelimDoaa M.EL-MekkawiReham M.M.AboeleninSohair A.Sayed AhmedGhada M.Mohamed, Preparation and characterization of Na-A zeolite from aluminum scrub and commercial sodium silicate for the removal of Cd^{2+} from water, Journal of the Association of Arab Universities for Basic and Applied Sciences, Volume 24, October 2017, Pages 19-25.
[20] A. Shoumkova, V. Stoyanova, SEM–EDX and XRD characterization of zeolite NaA, synthesized from rice husk and aluminium scrap by different procedures for preparation of the initial hydrogel, J. Porous Mater. 20 (1) (2013) 249–255.